Long-term comparison between the Japanese sardine *Sardinops melanostictus* stock level and simulated zooplankton density around the Kuroshio region

Haruka Nishikawa[1],*, Hiroyuki Tsujino[2,3], Shiro Nishikawa[1], Shin-Ichiro Nakayama[4], Hideyuki Nakano[2], Toru Sugiyama[1], Yoichi Ishikawa[1]

[1]Japan Agency for Marine-Earth Science and Technology (JAMSTEC), 3173-25 Showa-machi, Kanazawa-ku, Yokohama, Kanagawa 236-0001, Japan

[2]Meteorological Research Institute (MRI), Japan Meteorological Agency, Nagamine, Tsukuba, Ibaraki 305-0052, Japan

[3]Japan Meteorological Business Support Center, Chiyoda-ku, Tokyo 101-0054, Japan

[4]Japan Fisheries Research and Education Agency, Yokohama Laboratory, 2-12-4 Fukuura, Kanazawa-ku, Yokohama, Kanagawa 236-8648, Japan

ABSTRACT: Sardine species are known for multi-decadal-scale stock fluctuations. The Japanese sardine *Sardinops melanostictus* is one such species that is distributed near the Kuroshio western boundary current system. Like other sardines, food availability in the larval stage is thought to be an important factor in Japanese sardine stock fluctuations. Previous studies have suggested the significance of the feeding environment, particularly in the winter and spring seasons, within the Kuroshio axis area. However, collecting zooplankton, the primary food for larvae, along the strong current is challenging, and there is a lack of long-term observational data on zooplankton in this area. Therefore, in this study, we estimated zooplankton density in the Kuroshio axis area from 1967 to 2018 using a coupled physical—biological lower trophic level ecosystem model and compared it with the logarithm of recruitment per spawning stock biomass (LNRPS) and logarithm of recruitment per egg (LNRPE) of the Japanese sardine. Significant correlations were found between the zooplankton density and LNRPS from 1967 to 2004 and between zooplankton density and LNRPE from 1979 to 1996. Since, in this study, Granger causality was established between zooplankton density and LNRPS before 2005 and between zooplankton density and LNRPE before 1996, in these periods, namely 1967—2004 and 1979—1996, there is a high likelihood that zooplankton density influenced the interannual variation in recruitment. On the other hand, we found no relationship between recent food availability and LNRPS/LNRPE. This aspect remains a subject for future research.

KEY WORDS: Japanese sardine · Kuroshio · Stock fluctuation · Zooplankton · NPZD model

1. INTRODUCTION

The Japanese sardine *Sardinops melanostictus* is an important commercial fish in Japan. The spawning grounds are located along the Pacific coast of Japan, which is strongly influenced by the Kuroshio current from winter to spring (Kikuchi & Konishi 1990). Hatched larvae are transported by the Kuroshio current (Sugi-saki 1996, Kinoshita 1998), which then migrate northward in the Kuroshio—Oyashio transition region (Ivanov 1992). In autumn, they migrate southward from the Oyashio to the Kuroshio region for overwintering (Fig. 1) (Furuichi et al. 2022). Japanese sardine undergo drastic and multi-decadal stock fluctuations (e.g. Ito 1961, Yasuda et al. 1999). In the 20th century, Japanese sardine showed 2 peaks in the stock, during

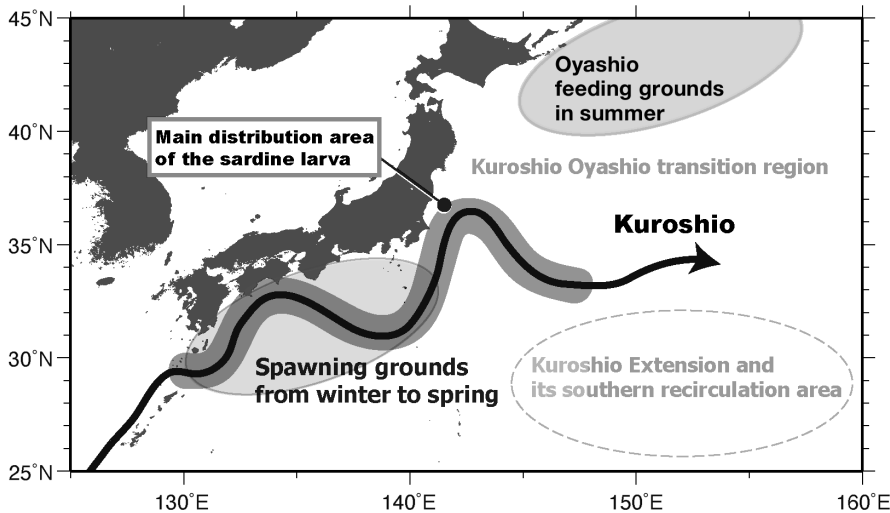*Corresponding author: harukan@jamstec.go.jp

Fig. 1. Spawning grounds of Japanese sardine from winter to spring, main distribution area from winter to spring, summer feeding grounds, and related regions. The curved black arrow represents the Kuroshio axis

the 1930s and the 1980s (Fig. 2) (Kawasaki 1983, Ministry of Agriculture, Forestry and Fisheries Japan 2023). The largest landing during the last high-stock period was 4.49 million tons in 1988, after which the catch decreased rapidly. Watanabe et al. (1995) attributed this drastic fluctuation in stock to large recruitment variability, especially with regards to the survival rate from the end of first-feeding larvae to age-1. Noto & Yasuda (1999, 2003) reported a relationship between larval mortality and winter–spring sea surface temperature (SST) in the Kuroshio Extension and its
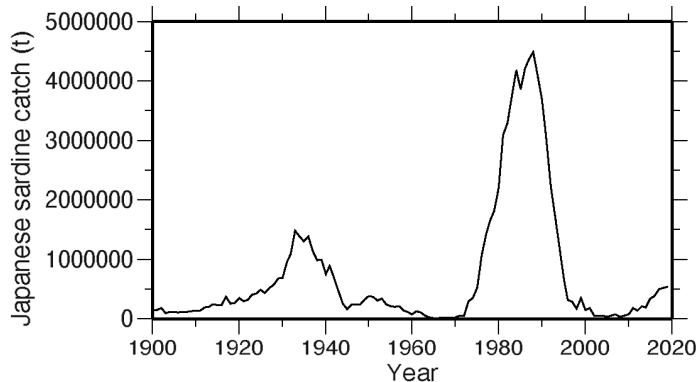

Fig. 2. Catch of Japanese sardine in Japan from 1900 to 2019. Catch data were obtained from a stock assessment report (Furuichi et al. 2022) and statistics on marine fishery production (Ministry of Agriculture, Forestry and Fisheries, Japan). Data before 1974 were compiled by Dr. Sho Furuichi from older statistics (Portal Site of Official Statistics of Japan [e-Stat]; https://www.e-stat.go.jp/stat-search/files?page=1& toukei=00500216&tstat=000001015174, https://www.e-stat.go.jp/stat-search/files?page=1&layout=datalist&toukei=00500216&tstat=000001015174&cycle=0&tclass1=0000010 34726&tclass2val=0)

southern recirculation area (145–180° E, 30–35° N). While those studies suggested an influence of the ocean environment on the sardine stock fluctuation, the Kuroshio Extension and its southern recirculation area are far away from the spawning grounds (Fig. 1), and no larvae have been found there so far. Nishikawa et al. (2011) focused on the environment of the Kuroshio axis area and found a negative correlation between the winter–spring SST and the logarithm of recruitment per spawning stock biomass (LNRPS) and a positive correlation between the winter mixed layer depth (MLD) and the LNRPS. These correlations strongly suggest that the larval habitat environment controls the sardine stock fluctuation via larval survival.

Two hypotheses have been proposed to explain the impact of SST or MLD on larval survival. One is the optimal growth temperature hypothesis (Takasuka et al. 2007), which indicates that the larval growth rate is highest at 16.2°C. Since 16.2°C is at the lower end of the temperature range in the area where sardine larvae are mainly distributed, low SST is related to high survival rate via the growth rate. The other hypothesis focuses on the winter MLD. Several previous studies have suggested that the Japanese sardine stock is influenced by food availability associated with vertical mixing variation (Polovina et al. 1995, Kasai 1996, Noto & Yasuda 2003, Yatsu et al. 2008, Nishikawa et al. 2013b). With regard to the larval distribution area, a model simulation study demonstrated that variation in the winter MLD can change spring primary production (Nishikawa & Yasuda 2008), and an observational study revealed that the MLD affects the chlorophyll *a* (chl *a*) concentration (Itoh et al. 2015). Thus, the correlation between MLD and LNRPS may reflect the influence of variation in food availability driven by bottom-up control. Additionally, it has been suggested that bottom-up control also influences the variability in sardine abundance in the Sea of Japan (Ohshimo et al. 2009).

The food availability hypothesis is not supported by the available food data. Sardine larvae feed on copepod nauplii (Uotani et al. 1988, Morimoto et al. 2023); however, long-term zooplankton observational data in the waters of Japan are scarce, except for the Odate collection in the Kuroshio–Oyashio transition region (Odate 1994). Therefore, while the significance of zooplankton biomass in relation to stock fluctuations for numerous small pelagic fish has been emphasized,

studies on stock fluctuations have often used chlorophyll concentration as an indicator of the feeding environment (e.g. Ichii et al. 2018 for *Cololabis saira*; Liu et al. 2020 for *Engraulis japonicus*). Especially in regions influenced by strong currents such as the Kuroshio, plankton collection is not easy, and although some data from line observations crossing the Kuroshio exist (Nakata & Hidaka 2003), there is a lack of long-term observational data covering the winter—spring Kuroshio axis region, which is the focus of this study.

Sardine species are distributed around the California, Humboldt, South Africa, and Kuroshio region. Interestingly, all of them show multi-decadal-scale stock fluctuations (Lluch-Cota 2013). Most of these regions are known for strong upwelling (e.g. Chavez & Messié 2009), while the Kuroshio region and the habitat of the Indian Ocean stock in South Africa are characterized by strong western boundary currents (Teske et al. 2021, Sakamoto et al. 2022). Long-term zooplankton data are available for upwelling regions such as Benguela and California, where it is known that the intensity of upwelling affects sardine stock fluctuation through changes in zooplankton biomass (Shannon et al. 2004, Rykaczewski & Checkley 2008). The question of whether the influence of food also exists in strong western boundary currents remains a highly intriguing issue.

In this study, we reproduced the zooplankton density in the larval habitat from 1967 to 2018 using a coupled physical—biological lower trophic level ocean ecosystem model and compared the zooplankton density with the LNRPS to validate the food availability hypothesis. There are 2 important highlights of our study: (1) it is the first to provide a comparison between LNRPS and zooplankton density, and (2) our analysis includes both stock-increasing and stock-decreasing periods. The end of the 1960s to the early 1970s is thought to be an important period for stock fluctuation (Kuroda 2005). We expected that something happened that resulted in the large catch after the 1970s (Fig. 2). However, no studies have examined the sardine stock fluctuation in the 1970s from the perspective of food availability except in the Kuroshio—Oyashio transition region (Okazaki et al. 2019).

Recently, a coupled physical—biological model that reproduces physical conditions by using observed atmospheric conditions from 1958 to 2018 was developed (Tsujino et al. 2024); it is a type of 'nutrient, phytoplankton, zooplankton, and detritus' (NPZD) model. NPZD models follow the flow from nutrient sources via trophic transfer to zooplankton (i.e. nutrient uptake by phytoplankton to zooplankton grazing on phytoplankton). Based on the physical model of Tsujino et al. (2024), the coupled NPZD model in our study was used to calculate zooplankton density including the previously unexplored data for the 1970s. One important feature of this model is the high spatial resolution, which can resolve the Kuroshio axis position that is necessary for the investigation of the feeding environment of Japanese sardine larvae. Using this model, we conducted the first study that compared the LNRPS and the logarithm of recruitment per egg (LNRPE) to the larval feeding environment over multiple decades, including stock-increasing and -decreasing periods.

2. DATA AND METHODS

2.1. LNRPS and LNRPE data

Recruitment per spawning stock biomass (RPS) is used as an index of survival from hatching to recruitment, and many studies have tried to explain the interannual variation in RPS by environmental fluctuations (Takasuka et al. 2007, Kuroda et al. 2020, Sakuramoto 2021). However, if there is a maternal effect, RPS varies depending on the spawning stock biomass—egg number relationship, and there is a possibility that the nutritional status of adults may also be reflected in recruitment. Takasuka et al. (2021) found a maternal effect for Japanese sardine and suggested that recruitment per egg (RPE) is more appropriate than RPS when comparing the feeding environment during the larval stage and recruitment.

We used both RPS and RPE in this study as indexes of survival from hatching to recruitment because the available RPE data set from 1979 to 2015, which was obtained from Takasuka et al. (2021), is too short to compare with the environment from the end of the 1960s. On the other hand, RPS data were estimated after 1951, but the data are not consistent. There are 2 available RPS data sets: one includes data from 1951 to 2000, estimated by a forward simulation approach fitted to egg production data (Wada & Jacobson 1998, Yatsu et al. 2005); the other includes data since 1976 that were estimated by a virtual population analysis by the Japanese Fisheries Research and Education Agency (Furuichi et al. 2022). Since a previous study (Yatsu et al. 2005) combined the 2 data sets for a long-term analysis, we also decided to combine the 2 RPS data sets. RPS data from 1967 to 2000 were obtained from Yatsu et al. (2005) and data from 1976 to 2018 were obtained from Furuichi et al. (2022). The means ± SD within the overlapping period of data (1976—2000)
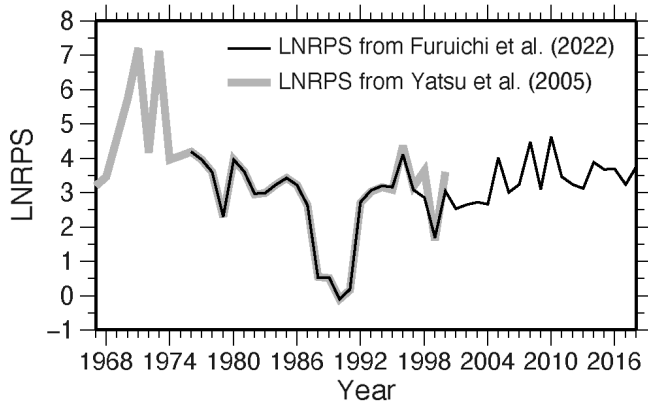
Fig. 3. Timeseries for the logarithm of recruitment per spawning stock biomass (LNRPS) derived from Furuichi et al. (2022) from 1976 to 2018 (black line) and derived from Yatsu et al. (2005) from 1967 to 2000 (gray line)

were 2.78 ± 1.26 for Yatsu et al. (2005) and 2.72 ± 1.22 for Furuichi et al. (2022) (Fig. 3). The correlation coefficient between the 2 data sets was 0.99, indicating that there was almost no difference between them. We logarithmically transformed the RPS and RPE and compared them with the environmental factors.

2.2. Ocean model

We used the ocean component of the Meteorological Research Institute Earth System Model version 2 (MRI-ESM2; Yukimoto et al. 2019) as the base global ocean model whose performance in terms of physical field was assessed by Urakawa et al. (2020). The source code was taken from Meteorological Research Institute Community Ocean Model version 4 (MRI.COMv4; Tsujino et al. 2017). To focus on the North Pacific Ocean, we embedded a high-resolution regional model for the North Pacific Ocean into the base global model. The domain for the regional model is 99° E–85° W zonally and 15° S–63° N meridionally. The horizontal resolution is 1/11° and 1/10° for zonal and meridional directions, respectively. The same 60 vertical levels as in the global model are used, and the biogeochemical cycle is included in the model. The biogeochemical processes consist of a carbon cycle model with carbonate chemistry and surface gas exchange parameterization that follow the protocols of OMIP-BGC (Biogeochemical protocols and diagnostics for the CMIP6 Ocean Model Intercomparison Project, Orr et al. 2017) and a simple NPZD-type ocean ecosystem model as used by Nakano et al. (2011, 2015). After a long-term spin-up for about 1500 yr, the global model was forced by repeating (6 times) the interannually varying atmospheric state from the 61 yr

JRA55-do data set from 1958 to 2018. The embedding of the high-resolution North Pacific Model within the global model started in the year 1998 of the fifth repeated cycle of the interannual forcing, which corresponds to the year 1937 relative to the start of the sixth cycle (1958). The model was integrated to the year 2018. The details of the model are shown in Tsujino et al. (2024). The output data are recorded monthly, so to create daily data from monthly data, linear interpolation was conducted.

To check the reproducibility of this model near the Kuroshio axis area, we compared the interannual variations of the simulated January–April SST with the ocean re-analysis data set FORA-WNP (Usui et al. 2017) and compared the January–April phytoplankton with MODIS-AQUA satellite data (https://oceancolor.gsfc. nasa.gov). The model phytoplankton concentration (mmol m^{-3}) was converted into chl a concentration using a ratio of 1.59 g chl a per mole of nitrogen (Hurtt & Armstrong 1996). We averaged the SST and phytoplankton density in the area with ±0.5° from the Kuroshio axis from 130 to 160° E during 1982–2015 for SST and during 2003–2015 for phytoplankton density. Although a previous study suggested that interannual variation in winter MLD affects the feeding condition via bottom-up control (Nishikawa et al. 2013b), observational MLD data for the Kuroshio axis area that suggest the possibility of interannual variation affecting the feeding condition are not available. Since interannual SST variation is closely related to the interannual MLD variation (Nishikawa & Yasuda 2011), we focused on the reproducibility of the interannual SST variation. FORA-WNP employs a 4-dimensional variational method for the data-assimilation system at the eddy-resolving level in the Northwestern Pacific. Because of the assimilation of the temperature–salinity profile through the data period and sea surface height (SSH) data from the satellite altimeter after 1993, FORA-WNP can reproduce the observed Kuroshio path that varies drastically within a few weeks. For this reason, FORA-WNP provides the most reliable data for determining the long-term SST variability near the Kuroshio axis.

We were interested in determining the density of nauplii along the route where larvae are transported by the Kuroshio. However, it is challenging to collect plankton samples extensively along the fast-flowing Kuroshio axis, and as a result, no such observational data are available. Therefore, we compared the observational data from a location that is not directly on the path of the Kuroshio, but relatively close to it, with the model. Nakata & Hidaka (2003) estimated the copepod biomass in the Kuroshio area from 1971 to 2000. Their observations were conducted along multiple meridians

crossing the Kuroshio axis. From February to March, copepods were collected along the meridian at 136—139° E, starting from a location where the water temperature was 15°C at 200 m depth, up to a location where the surface current velocity was below 2 knots. These environmental indicators closely correspond to the Kuroshio's strong current zone. Collection was conducted by vertical tows with ring nets (diameter 45 or 60 cm; mesh size 0.33 mm) from 150 m to the surface. Zooplankton were aggregated and divided into 2 categories based on their prosomal lengths: large (lengths ⩾1 mm) and small (<1 mm). Using the same definition, observation points were determined in the model, and the yearly averaged concentration of zooplankton in the area was examined. Since the model considers only one type of zooplankton, the average concentration of zooplankton was compared with the biomasses of both the larger and smaller copepods.

2.3. Feeding environment

From the ocean model, we determined the zooplankton density in the upper layers. The main prey of sardine larvae are copepod nauplii, but we regarded the zooplankton density as the index of food availability. We averaged the zooplankton density in the 0—30 m layer according to the observed larval distribution data (Tsukamoto et al. 2001). Before metamorphosing to the juvenile stage that occurs about 2 mo after hatching (Kuroda 1991), the swimming ability of the larvae is poor and thus negligible.

Since the spawning grounds are usually located near the Kuroshio axis, the eggs and larvae are dispersed by the Kuroshio, which drastically varies its path within

a few weeks. For this reason, it is difficult to define the larval feeding grounds based on latitude and longitude. Thus, previous studies treated larvae as passively transported particles and determined the larval distribution area by using particle-tracking experiments from the spawning grounds (Itoh et al. 2009, Nishikawa 2019). This study also followed these methods and conducted particle-tracking experiments. Unfortunately, organized spawning ground data with the same reliability as the spawning ground survey results after 1978 are not available. To reproduce the past feeding environment, we released 5962 particles at 0.1° intervals (zonally and meridionally) in the area 130—141° E, 29—36° N, where spawning often occurred historically (Nishikawa 2019) and tracked their position, temperature at 200 m depth, and zooplankton density from 0 to 30 m at each position for 60 d. We then selected only the particles that were transported along the Kuroshio based on the report that the environment near the Kuroshio axis area is strongly affected by interannual variation in the LNRPS (Nishikawa 2019). The definition of transportation along the Kuroshio is as follows: (1) The longitude at 60 d post release is removed from the initial longitude by 10° or more. (2) The mean temperature at 200 m depth during the 60 d is above 10°C and below 21°C. The Kuroshio axis is generally located in a place where the water temperature is around 14—15°C at a depth of approximately 200 m (Kawai 1972). Considering the significance of locations within 0.5—1° latitude north and south of the Kuroshio axis as the feeding environment (Nishikawa 2019), we examined the water temperature at 200 m within 1° latitude north and south of the flow axis. Since the temperature at this location ranged from 10 to 21°C, criterion (2) was applied. Fig. 4 presents an example of the paths of
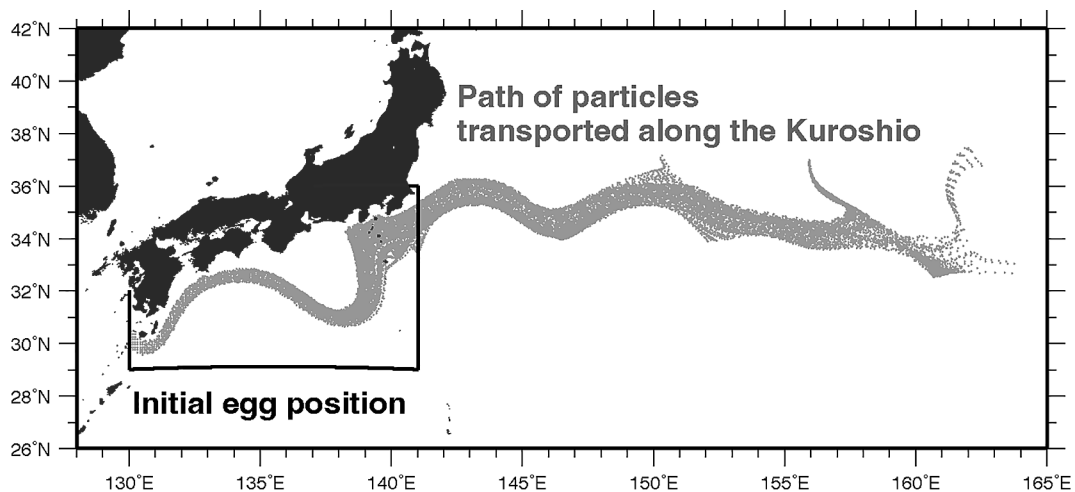

Fig. 4. Example of the simulated daily positions of particles transported along the Kuroshio. These particles were released from the boxed area on 15 February 1970 in the velocity field that was simulated by Tsujino et al. (2024)

selected particles. The particles were released in the upper 7 layers (depth from 0.5 to 26 m) on every 15th day from January to April for the period 1968–2018. January–April is the main spawning season of Japanese sardine (Nishikawa 2019). We considered the first 10 yr of the simulation, from 1958 to 1967, as a spin-up period and did not include it in the analysis. Previous particle-tracking experiments for Japanese sardine eggs and larvae compared the influence of the horizontal diffusion coefficient on dispersion and concluded that the results are almost the same at a horizontal diffusion coefficient ranging from 0 to 100 $m^2 s^{-1}$ (Nishikawa et al. 2013a). According to this result, we did not consider horizontal diffusion in this study. Thus, particle locations were traced as follows:

$$x_{n,t+1} = x_{n,t} + u_{n,t}\Delta t \qquad (1)$$

$$y_{n,t+1} = y_{n,t} + v_{n,t}\Delta t \qquad (2)$$

where $(x_{n,t}, y_{n,t})$ is the horizontal location of the nth particle (x and y are east–west and north–south coordinates, respectively) at time step t; $u_{n,t}$ and $v_{n,t}$ are the eastward and northward velocities from the physical model, respectively; and Δt is the time step. Finally, we averaged the ambient zooplankton density and water temperature from 0 to 30 m depth and from the day of release to the last day of the simulation for all particles that are transported along the Kuroshio every year. These yearly zooplankton density and temperature values were compared with the LNRPS/LNRPE as the feeding environment by using the t-test.

2.4. Data analysis

As correlation does not imply causation, observing simple correlations is not sufficient to comment on causality. To evaluate the possibility that the amount of zooplankton drives the efficiency of sardine recruitment, we conducted the Granger causality test (Granger 1969) in addition to correlation analysis. The Granger causality test is a statistical hypothesis test for determining whether one time series has a predictive causality on another time series. Although even the Granger causality test is not sufficient to perfectly detect actual causalities (Granger 1969), the amount of zooplankton becomes more likely to drive the LNRPS/LNRPE of sardine if Granger causality is detected between the 2 time series.

The Granger causality test was performed following Granger (1969) and Okimoto (2010), based on vector autoregressive (VAR) and autoregressive (AR) models: Model A estimates LNRPS for year y based on the previous year's LNRPS and the current year's zoo-

plankton density, and Model B explains LNRPS for year y using only the previous year's LNRPS ($c_1 - c_5$, and $c_6 - c_8$ in Model C below, are constants):

$$LNRPS_y = c_1 \cdot LNRPS_{y-1} + c_2 \cdot zoo_y + c_3 \qquad \text{(Model A)}$$

$$LNRPS_y = c_4 \cdot LNRPS_{y-1} + c_5 \qquad \text{(Model B)}$$

Because adding new explanatory variables certainly improves the model fit, we performed an F-test to evaluate whether the progress of the fit in Model A is significant. The F-value is expressed as in Eqn. (3) using the sum of squared residuals when estimating $LNRPS_y$ in Model A, denoted as SSR_1, and the sum of squared residuals in Model B, denoted as SSR_0. Here, T represents the sample size:

$$F = \frac{\left(SSR_0 - SSR_1\right)/2}{SSR_1 /\left(T - 5\right)} \qquad (3)$$

Taking LNRPS data from 1967 to 2018 as an example, we predicted LNRPS by determining the best-fitting coefficients for each model, Models A and B, for each year from 1968 to 2018. We then calculated the F-value to conduct the F-test. In this study, we applied the Granger causality test to zooplankton and LNRPS/LNRPE time series, whose durations were 1967–1997, 1967–1998, ..., 1967–2018 and 1976–1997, 1976–1998, ..., 1976–2018 for LNRPS, and 1979–1994, 1979–1995, ..., 1979–2015 for LNRPE. There are 2 reasons why we did not analyze only a single period, i.e. either 1967–2018 or 1979–2015. One is that a previous study reported that the growth–recruitment relationship has disappeared since the late 1990s (Furuichi et al. 2020), which implies that the effect of zooplankton on LNRPS/LNRPE has recently become weak and therefore might prohibit the detection of Granger causality that actually existed in the past. The other reason is that we combined 2 types of LNRPS. Since the reliability of the LNRPS before 1975 may be low, we conducted a Granger causality test as a precaution for the period after 1976.

In addition, we need to consider the 'backdoor' path underlying the connection between zooplankton density and recruitment. Recruitment is believed to be influenced by both zooplankton and water temperature, but temperature acts as a confounding factor that affects both plankton productivity and recruitment through fish physiology. While temperature influences recruitment by controlling the growth rate, which depends on the fish metabolic rate (Takasuka et al. 2007, Sakamoto et al. 2022), it also has an influence on plankton. Low temperatures cause strong vertical mixing and nutrient supply, resulting in increased phytoplankton and zooplankton (Nishikawa et al. 2013b).

Additionally, factors related to the fluctuations in phytoplankton and zooplankton density, such as photosynthesis, predation rates, and mortality rates, are also influenced by water temperature (Nakano et al. 2011, 2015). Fig. 5 illustrates the relationship among the water temperature, zooplankton density, and recruitment. Therefore, even if zooplankton density has Granger causality with LNRPS/LNRPE, it is not possible to exclude the possibility of a water temperature influence caused by physiological and metabolic effects.

In this study, we also conducted a Granger causality test for the water temperature with respect to LNRPS/ LNRPE. While it is considered that water temperature also has Granger causality, if the p-value from the VAR model estimated using zooplankton density is lower than the p-value from the VAR model estimated using water temperature, it suggests that predictions using zooplankton are more accurate, which implies a higher likelihood of the direct impact of zooplankton itself. Since there is a dome-shaped relationship between water temperature and the growth rate of larvae (Takasuka et al. 2007), we took into account the effect of the quadratic term of temperature as follows:

$$\mathrm{LNRPS}_y = c_5 \cdot \mathrm{LNRPS}_{y-1} + c_6 \cdot \mathrm{Temp}_y + c_7 \cdot \mathrm{Temp}_y^2 + c_8$$
$$\text{(Model C)}$$

The Granger causality test for water temperature was based on the comparison between Models B and C.

3. RESULTS

3.1. Reproducibility of the model

The January, February, March, and April SST interannual variation from the present use model shows positive correlations (r = 0.62, 0.67, 0.70, and 0.71,

respectively) with that from the FORA-WNP (Fig. 6). All correlation coefficients are statistically significant at a significance level of 0.2% (n = 24, *t*-test). These results suggest that the interannual variation in SST near the Kuroshio axis from the model is mostly same as indicated by the FORA-WNP data.

For phytoplankton density, the correlation coefficients between the model and satellite data from January to April are 0.73, 0.71, 0.45, and 0.73 (Fig. 7). Except for March, correlation coefficients are statistically significant at a significance level of 0.6% (n = 13, *t*-test). March shows a consistent trend between model and satellite data, with higher agreement in 2003−2005 and 2012, and lower agreement in 2006−2008. However, the trend in 2005 differs significantly at a significance level of 10% (Fig. 7c). Unlike SST, in the case of phytoplankton density, even when the temporal trends of the model values are similar to the observed values, the means and standard deviations differ. From February, there is a notable trend of smaller standard deviations in the model values. For example, in April, the model value is 0.56 ± 0.02 mg m^{-3}, while the observed value is 0.49 ± 0.12 mg m^{-3}, indicating a significantly smaller model standard deviation.

For the winter zooplankton concentration in the Kuroshio region, the correlation coefficients between the model zooplankton concentration and observed large zooplankton biomass, as well as observed small zooplankton biomass, were 0.54 (p < 0.005) and 0.22, respectively. A significant correlation was only observed between the model zooplankton concentration and observed large zooplankton biomass (Fig. 8). The temporal trends of the model and observed large zooplankton biomass were in agreement, with high levels during 1971−1979, low levels in the 1980s, and a subsequent increasing trend during the 1990s (Fig. 8a).
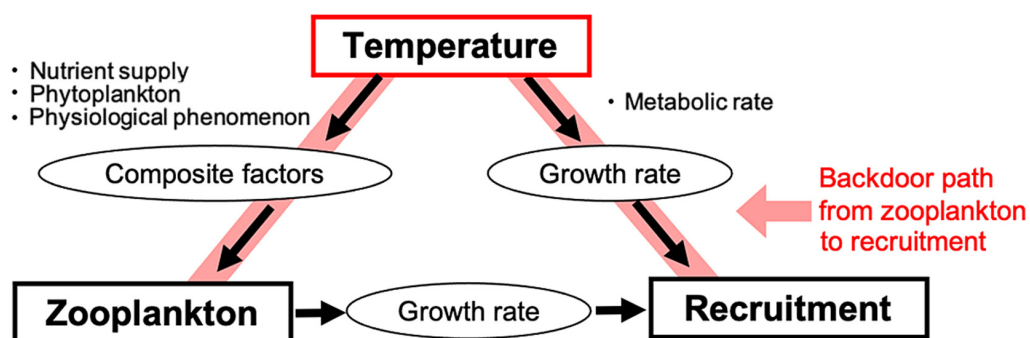

Fig. 5. Relationship among water temperature, zooplankton density, and recruitment. Both temperature and zooplankton density affect recruitment through growth rate. However, temperature also affects zooplankton density through nutrient supply. When considering the path that influences recruitment from zooplankton, it is important to note that temperature does not act independently on recruitment but acts as a confounding factor positioned upstream of zooplankton. Thus, attention must be paid to the existence of the 'backdoor' path from zooplankton to recruitment, which is represented by black arrows with a red shadow
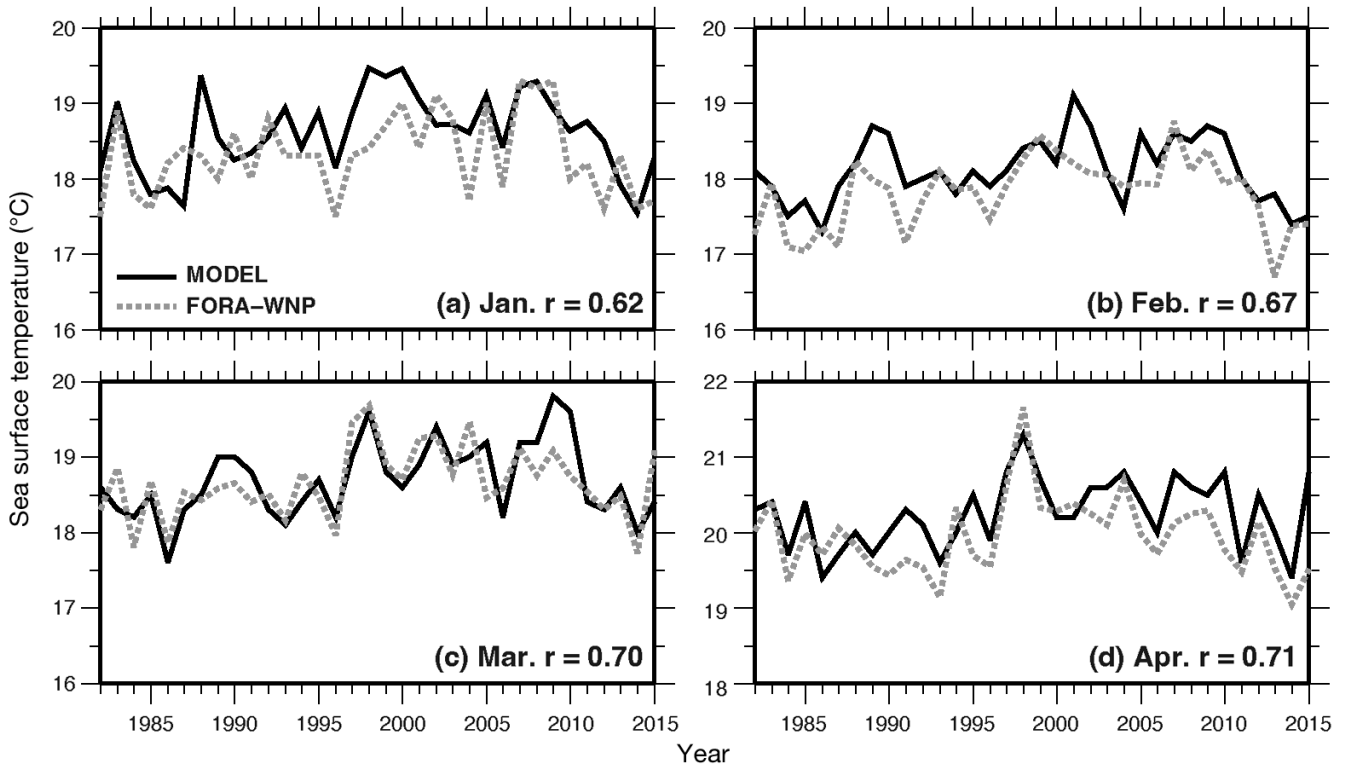
Fig. 6. Time series of the (a) January, (b) February, (c) March, and (d) April sea surface temperature (SST) around the Kuroshio axis area from the Tsujino et al. (2024) model (black solid line) used in this study and from the re-analysis data set FORA-WNP (gray dotted line) from 1982 to 2015. r: correlation coefficient
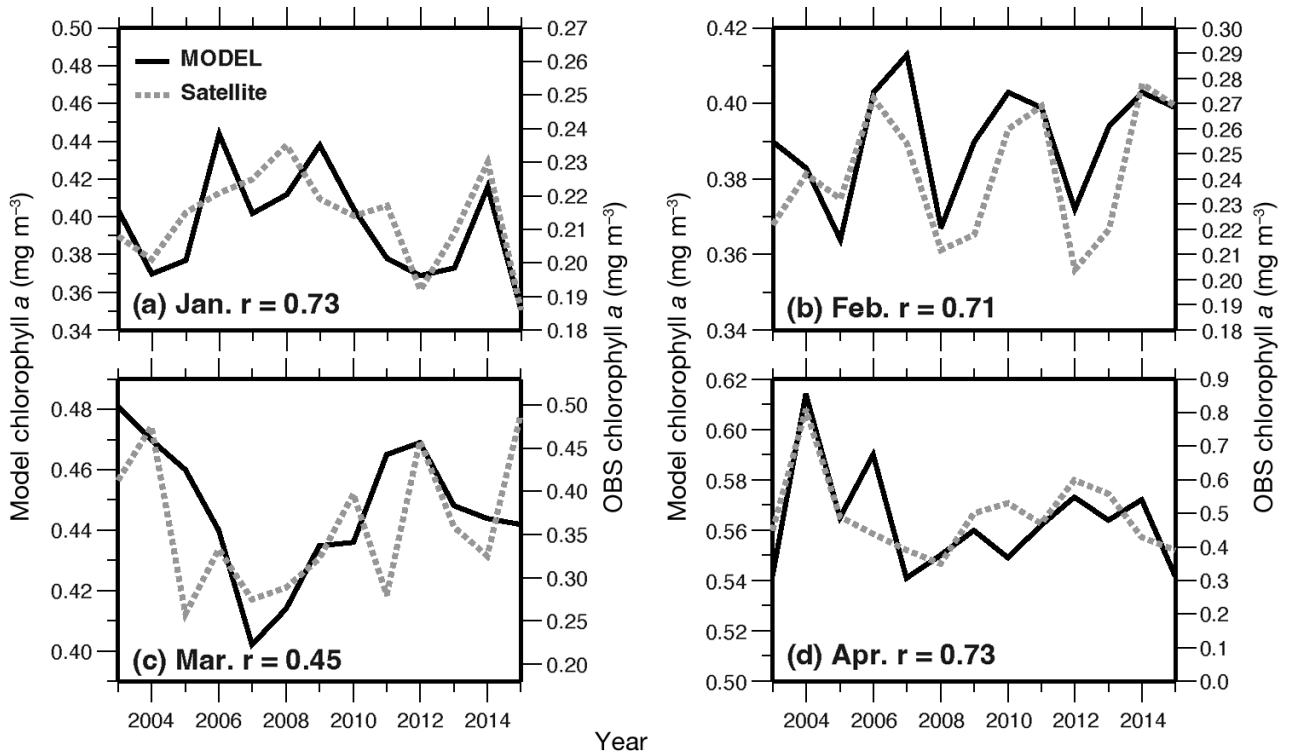

Fig. 7. Time series of the (a) January, (b) February, (c) March, and (d) April chl *a* around the Kuroshio axis area from the Tsujino et al. (2024) model (black solid line) used in this study and from the MODIS-AQUA satellite data (https://oceancolor. gsfc.nasa.gov; gray dotted line) from 2003 to 2015. r: correlation coefficient
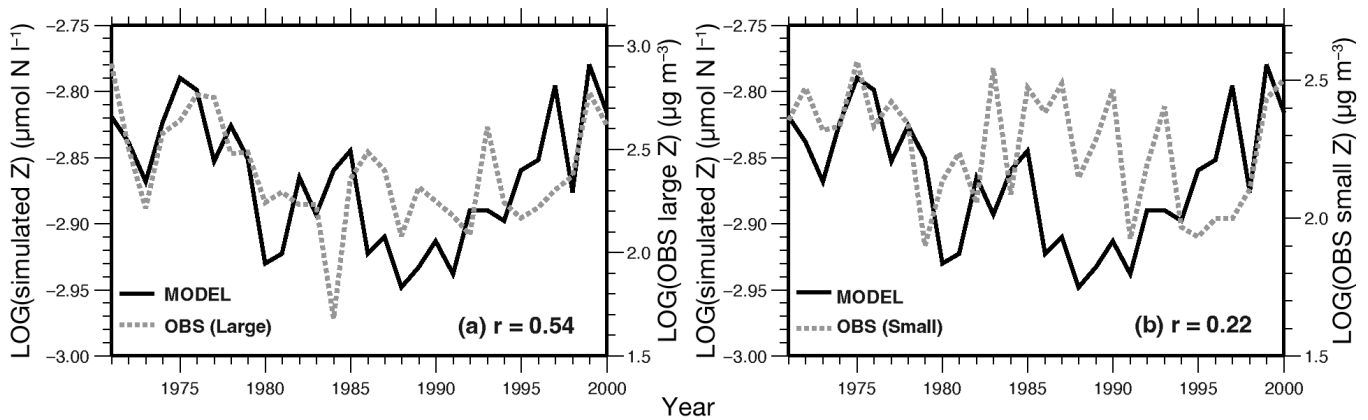
Fig. 8. Time series of the zooplankton density from the model (Tsujino et al. 2024, black solid line and left-hand scale) and observed biomass of (a) large zooplankton (prosomal lengths >1 mm) and (b) small zooplankton (prosomal lengths <1 mm) (gray dotted line) from 1971 to 2000 in the Kuroshio region (136—139° E). Observed zooplankton data are derived from Nakata & Hidaka (2003). Both density and biomass are log-transformed. r: correlation coefficient

3.2. LNRPS/LNRPE vs. simulated zooplankton density

There is a significant positive correlation (r = 0.58, p < 0.01, n = 52) between the LNRPS and simulated zooplankton in the main feeding grounds of the Japanese sardine larvae (Fig. 9). We especially focused on 2 periods, from the late 1960s to the 1970s and around the end of the 1980s, which were periods when the stock increased and decreased, respectively (Fig. 2). The mean LNRPS and mean zooplankton density from 1967 to 2018 were 3.31 and 3.15 nmol l^{-1}, respectively. From late 1968 to 1978, LNRPS and zooplankton density were consistently greater than the
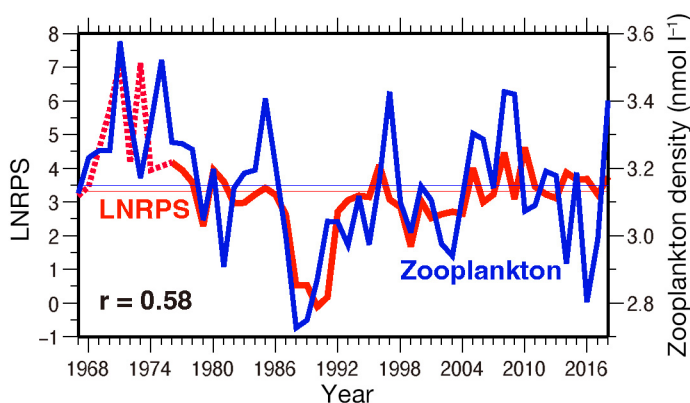

Fig. 9. Time series of the LNRPS (red solid and dotted lines and left-hand scale) and simulated zooplankton density near the Kuroshio axis (blue line and right-hand scale) from 1967 to 2018. The LNRPS was derived from Yatsu et al. (2005) (dotted line) and Furuichi et al. (2022) (solid line). The red and blue horizontal lines are the mean LNRPS (3.31) and mean zooplankton density (3.15 nmol l^{-1}), respectively. r: correlation coefficient

mean value. The highest LNRPS value (7.19) was recorded in 1971, when the highest zooplankton density (3.58 nmol l^{-1}) was recorded. From 1988 to 1991, the LNRPS was remarkably low, and the zooplankton density was also below the mean value. The lowest and second lowest zooplankton density values were recorded in 1988 and 1989, respectively.

In the period from the 1990s to the early 2000s, values of LNRPS and zooplankton density above the mean values were only recorded in 1996 and 1997, respectively. After 2005, both LNRPS and zooplankton density often exceeded the mean value, but the interannual variations were not always coincident. When dividing the correlation period, the correlation coefficient (r) is 0.62 (p < 0.001, n = 26) for 1979—2004. However, for 2005—2015, the correlation coefficient becomes −0.09 (n = 11), and a positive correlation is no longer observed after 2005.

When examining the correlation between simulated zooplankton and LNRPE in the period from 1979 to 2015, no significant correlation was found (Fig. 10) (r = 0.22, n = 37). When dividing the correlation period, a significant positive correlation was observed for 1979—1996 (r = 0.55, p = 0.02, n = 18), and although not significant, a negative correlation was seen for 1997—2015 (r = −0.16, n = 19). This relationship is similar to that observed between LNRPS and the simulated zooplankton. LNRPE showed a tendency to be higher than average from 1979 to 1987 (except for 1981), and lower than average from 1987 to 1995 within the period 1979—2015.

Zooplankton density exhibited Granger causality with respect to LNRPS prediction during any period from 1967—1997 to 1967—2018 (Table 1). The p-values were lowest during the period from 1967—2005 to
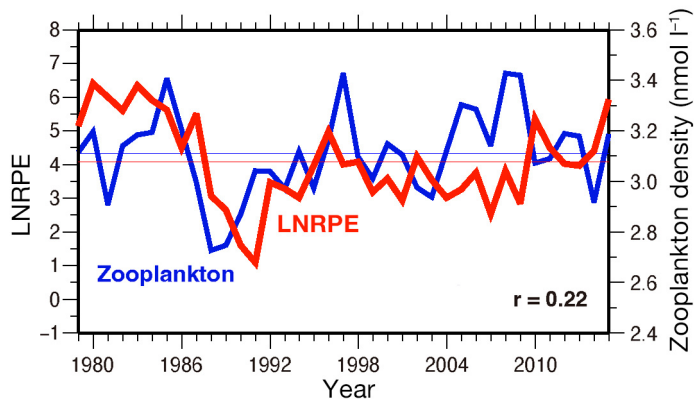
Fig. 10. Time series of the logarithm of recruitment per egg (LNRPE) (red line and left-hand scale) and simulated zooplankton density near the Kuroshio axis (blue line and right-hand scale) from 1979 to 2015. RPE is derived from Takasuka et al. (2021). The red and blue horizontal lines are the mean LNRPE (4.09) and mean zooplankton density (3.11 nmol l^{-1}), respectively. r: correlation coefficient

Table 1. 2F- (double F values) and p-values for Granger causality tests of the vector autoregressive (VAR) model estimating the logarithm of recruitment per spawning stock biomass (LNRPS) from zooplankton density for 22 time periods from 1967–1997 to 1967–2018. *Null hypothesis of no Granger causality rejected

Time period	2F	p	Time period	2F	p
1967–2018	8.396	0.005*	1967–2007	10.97	0.001*
1967–2017	8.027	0.006*	1967–2006	10.67	0.002*
1967–2016	7.774	0.006*	1967–2005	11.17	0.001*
1967–2015	9.221	0.003*	1967–2004	9.797	0.003*
1967–2014	9.017	0.003*	1967–2003	9.556	0.003*
1967–2013	10.70	0.002*	1967–2002	9.499	0.003*
1967–2012	10.49	0.002*	1967–2001	9.323	0.003*
1967–2011	10.27	0.002*	1967–2000	8.973	0.002*
1967–2010	9.589	0.003*	1967–1999	8.262	0.006*
1967–2009	10.84	0.001*	1967–1998	7.476	0.008*
1967–2008	12.72	0.001*	1967–1997	7.160	0.010*

Table 2. As in Table 1, but for the VAR model estimating LNRPS from zooplankton density for 22 time periods from 1976–1997 to 1976–2018

Time period	2F	p	Time period	2F	p
1976–2018	6.893	0.010*	1976–2007	11.06	0.002*
1976–2017	6.098	0.016*	1976–2006	10.62	0.002*
1976–2016	5.930	0.017*	1976–2005	11.60	0.001*
1976–2015	7.835	0.007*	1976–2004	8.995	0.004*
1976–2014	7.623	0.007*	1976–2003	8.663	0.005*
1976–2013	10.25	0.002*	1976–2002	8.895	0.005*
1976–2012	9.953	0.002*	1976–2001	8.902	0.005*
1976–2011	9.664	0.003*	1976–2000	8.546	0.006*
1976–2010	8.986	0.004*	1976–1999	7.327	0.010*
1976–2009	11.59	0.001*	1976–1998	6.626	0.014*
1976–2008	14.62	0.001*	1976–1997	6.271	0.017*

1967–2009. These results are consistent with the correlation analysis, in which the correlation coefficients also decreased after 2005. When we used LNRPS after 1976, which is the new data set estimated by Japanese Fisheries Research and Education Agency (Furuichi et al. 2022), the Granger causality exists from 1976–1997 to 1976–2018 (Table 2). On the other hand, Granger causality was detected only during the period from 1979–1996 for LNRPE (Table 3). This result is also consistent with the correlation analysis.

3.3. LNRPS/LNRPE vs. simulated water temperature

There is a significant negative correlation (r = −0.40, p < 0.02) between water temperature along the main transport routes of sardine larvae and LNRPS (Fig. 11), whereas the correlation coefficient between water temperature and LNRPE is not significant (r = −0.21, p = 0.2) (Fig. 12). This trend is consistent with zooplankton density. The results of the Granger causality test indicate that, for the LNRPS after 1967, water temperature exhibited Granger causality for all periods except 1967–1997, 1967–1998, and 1967–2003 (Table 4). However, when comparing p-values for the same periods with zooplankton density (Table 1), they were all considerably higher. When we restricted the LNRPS period to after 1976, zooplankton exhibited Granger causality for the entire period (Table 2), whereas water temperature showed Granger causality for 9 out of 22 periods (Table 5). The Granger causality test for LNRPE indicated no Granger causality for any period (Table 6).

Table 3. As in Table 1, but for the VAR model estimating the logarithm of recruitment per egg (LNRPE) from zooplankton density for 22 time periods from 1979–1994 to 1979–2015

| Time period	2F	p	Time period	2F	p
1979–2015	3.986	0.235	1979–2004	4.062	0.122
1979–2014	3.991	0.272	1979–2003	4.073	0.110
1979–2013	3.996	0.231	1979–2002	4.085	0.139
1979–2012	4.001	0.237	1979–2001	4.098	0.117
1979–2011	4.007	0.234	1979–2000	4.113	0.108
1979–2010	4.013	0.247	1979–1999	4.130	0.122
1979–2009	4.020	0.195	1979–1998	4.149	0.141
1979–2008	4.027	0.079	1979–1997	4.171	0.154
1979–2007	4.034	0.147	1979–1996	4.196	0.041*
1979–2006	4.043	0.113	1979–1995	4.225	0.063
1979–2005	4.052	0.133	1979–1994	4.260	0.063
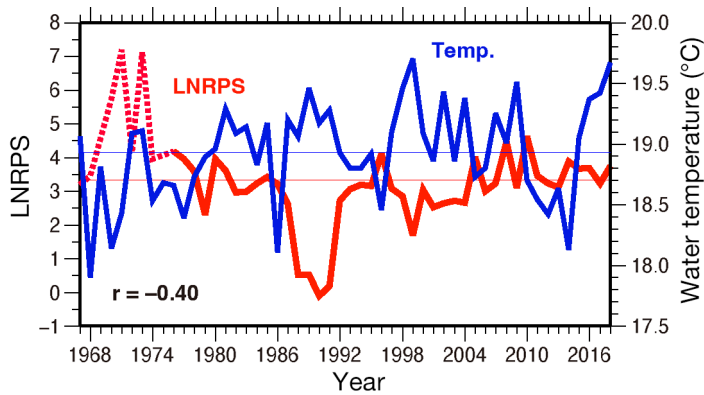
Fig. 11. Time series of the LNRPS (red solid and dotted lines and left-hand scale) and simulated water temperature near the Kuroshio axis (blue line and right-hand scale) from 1967 to 2018. The LNRPS was derived from Yatsu et al. (2005) (dotted line) and Furuichi et al. (2022) (solid line). The red and blue horizontal lines are the mean LNRPS (3.31) and mean temperature (18.93°C), respectively. r: correlation coefficient
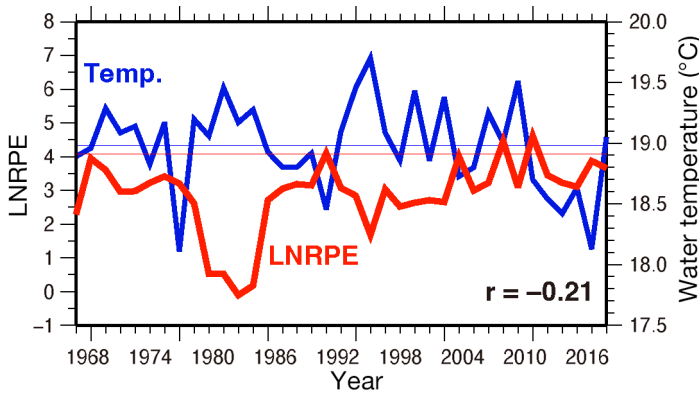

Fig. 12. Time series of the LNRPE (red line and left-hand scale) and simulated water temperature near the Kuroshio axis (blue line and right-hand scale) from 1979 to 2015. RPE is derived from Takasuka et al. (2021). The red and blue horizontal lines are the mean LNRPE (4.09) and mean temperature (18.98°C), respectively. r: correlation coefficient

Table 4. 2*F*- and p-values of the Granger causality test for the VAR model estimating LNRPS from water temperature for 22 time periods from 1967−1997 to 1967−2018. *Null hypothesis of no Granger causality rejected

Time period	2*F*	p	Time period	2*F*	p
1967−2018	4.021	0.047*	1967−2007	4.813	0.030*
1967−2017	5.710	0.018*	1967−2006	4.198	0.043*
1967−2016	6.126	0.015*	1967−2005	5.300	0.023*
1967−2015	6.408	0.013*	1967−2004	4.209	0.043*
1967−2014	6.222	0.014*	1967−2003	3.739	0.056
1967−2013	4.637	0.033*	1967−2002	4.352	0.040*
1967−2012	4.468	0.037*	1967−2001	4.364	0.040*
1967−2011	5.425	0.022*	1967−2000	4.103	0.046*
1967−2010	6.300	0.013*	1967−1999	4.460	0.038*
1967−2009	5.872	0.017*	1967−1998	3.258	0.075
1967−2008	4.086	0.046*	1967−1997	3.292	0.073

Table 5. As in Table 4, but for the VAR model estimating LNRPS from water temperature for 22 time periods from 1976−1997 to 1976−2018

Time period	2*F*	p	Time period	2*F*	p
1976−2018	3.612	0.060	1976−2007	4.571	0.036*
1976−2017	4.343	0.039*	1976−2006	4.015	0.049*
1976−2016	3.339	0.070	1976−2005	2.464	0.121
1976−2015	3.248	0.074	1976−2004	3.179	0.079
1976−2014	5.966	0.016*	1976−2003	2.961	0.090
1976−2013	2.436	0.122	1976−2002	3.969	0.050*
1976−2012	2.432	0.122	1976−2001	1.903	0.173
1976−2011	4.022	0.048*	1976−2000	3.387	0.071
1976−2010	4.359	0.040*	1976−1999	1.453	0.233
1976−2009	5.063	0.027*	1976−1998	2.645	0.110
1976−2008	4.489	0.037*	1976−1997	2.181	0.146

Table 6. As in Table 4, but for the VAR model estimating LNRPE from water temperature for 22 time periods from 1979−1994 to 1979−2015

Time period	2*F*	p	Time period	2*F*	p
1979−2015	1.329	0.252	1979−2004	1.115	0.295
1979−2014	2.261	0.136	1979−2003	0.496	0.484
1979−2013	1.855	0.177	1979−2002	0.966	0.330
1979−2012	1.408	0.239	1979−2001	0.593	0.445
1979−2011	1.181	0.280	1979−2000	1.717	0.196
1979−2010	2.585	0.112	1979−1999	1.069	0.306
1979−2009	1.859	0.177	1979−1998	0.032	0.858
1979−2008	1.289	0.260	1979−1997	0.957	0.334
1979−2007	0.658	0.420	1979−1996	0.525	0.473
1979−2006	0.970	0.328	1979−1995	0.272	0.605
1979−2005	0.370	0.545	1979−1994	0.001	1.000

4. DISCUSSION

4.1. Reproducibility of the model

The coupled physical−biological model successfully reproduced the interannual variation in SST. The correlation coefficients between the model and observations are significant at a significance level of 0.2% or less for all months. The interannual variation in chl *a* concentration was reproduced except for March. The reason for the lower reproducibility for March, compared to other months, is likely due to the dependence of chl *a* concentration in this month on the timing of the bloom. Until March, the mixed layer is deep, and the bloom occurs when the mixed layer becomes shallow in April. However, occasionally, when the mixed layer becomes shallow in March, phytoplankton starts to increase beginning in March, resulting in a decrease in phytoplankton concentration in April (Nishikawa & Yasuda 2008). The year 2005,

which exhibited particularly poor reproducibility, had observed chlorophyll values of 0.258 mg m^{-3} in March (compared to the 2003–2015 average of 0.359 mg m^{-3}; the same comparison applies hereafter) and 0.490 mg m^{-3} in April (compared to 0.493 mg m^{-3}). In contrast, the model simulation values were 0.460 (0.447) mg m^{-3} for March and 0.566 (0.560) mg m^{-3} for April (Fig. 6c,d). In 2005, in the real ocean, the mixed layer may have been thick; consequently, photosynthesis was inhibited until March, and phytoplankton did not increase. On the other hand, in the model simulation, the mixed layer was shallow in March, and photosynthesis became active at that time. As a result, unlike in reality, the model showed high phytoplankton density in March. The depth of the mixed layer depends on SST (Nishikawa & Yasuda 2011). In fact, the observed SST in March was 18.5°C, while the simulation showed a higher value of 19.2°C (Fig. 6c). As a result, there was a significant discrepancy in the simulated chlorophyll values for the year 2005.

Regarding zooplankton, there was a significant correlation (r = 0.54, p < 0.005) between large zooplankton biomass and the simulated zooplankton concentration, indicating that the model was able to reproduce the interannual variations. On the other hand, there was no correlation between small zooplankton biomass and the simulated zooplankton concentration. The reason why the interannual variations in large zooplankton and small zooplankton do not align can be attributed to the differences in their ecological characteristics, as explained by Nakata et al. (2001). Large algae, which serve as a food source for large zooplankton, depend on nutrients. Therefore, the growth and reproduction of large zooplankton also rely on surface nutrient concentrations, increasing in years with higher nutrient supplies from the subsurface. On the other hand, small zooplankton feed on small algae, which require fewer nutrients compared to large algae. As a result, the interannual variation in small zooplankton does not depend on nutrient supply. The ecosystem model used in this study is a simple model with one species of zooplankton and one species of phytoplankton. Therefore, in this area, the limiting factor for primary production is nutrient concentration, and the interannual variation is dependent on nutrient supply. In this regard, it is reasonable that the interannual variations of observed large zooplankton and simulated zooplankton match, as it indicates that the nutrient supply process is well reproduced in the model. On the other hand, evaluating the impact of the lack of reproducibility on the interannual variation of small zooplankton is difficult. In reality, it is believed that sardine larvae feed on both large and small zooplankton nauplii. However, since

the standard deviation of large zooplankton is twice that of small zooplankton, there is a possibility that large zooplankton has a greater influence on the interannual variations.

4.2. Feeding environment and LNRPS/LNRPE

The important results of this study are that the simulated zooplankton density tended to be high during the high LNRPS period from the late 1960s to the 1970s and the zooplankton density tended to be low during the low LNRPS/LNRPE period around the end of the 1980s. These results support the hypothesis that food availability near the Kuroshio axis area during the larval stage has an impact on recruitment. Although there is a significant positive correlation between the simulated zooplankton density and the LNRPS (1967–2004) and LNRPE (1979–1996), the yearly variation in zooplankton density does not always match the yearly variation in LNRPS/LNRPE during these periods, from the late 1960s to 1970 and the end of the 1980s. For example, the second largest LNRPS was recorded in 1973 but the second largest zooplankton density was recorded in 1975, and in 1991, LNRPS was low but the zooplankton density was not (Fig. 9). In addition, if we limit the period for correlation analysis to the years 2005 to 2015, there were no correlations between LNRPS/LNRPE and zooplankton.

It is very difficult to conclude that the feeding environment 'truly' has an impact on recruitment because there are backdoor paths as described in Fig. 5. While there was a significant negative correlation between LNRPS and zooplankton density, the possibility that this correlation resulted from temperature cannot be ruled out. Therefore, in this study, we evaluated the impact of zooplankton density itself on LNRPS by comparing the p-values of the Granger causality tests for zooplankton density and water temperature with respect to LNRPS. Firstly, water temperature exhibited Granger causality with LNRPS (Table 4). This result suggests that water temperature may influence recruitment through some pathway, as indicated in Fig. 5. If zooplankton itself does not impact recruitment, and the correlation between zooplankton and recruitment reflects only the backdoor path via water temperature (i.e. a spurious correlation), then the p-value for the influence of zooplankton on LNRPS should be larger than that for water temperature. However, the results showed that the p-value for the zooplankton model was smaller (Tables 1, 2, 4, 5). From this, it can be inferred that LNRPS is likely directly influenced not only by water temperature but

also by zooplankton density. It is noted that the water temperature VAR model (Model C) includes a quadratic term. Adding the quadratic term certainly improves the model fit; therefore, the smaller p-values obtained in the comparison of Models A and B indicate that the effect of zooplankton was detectable even if the effect of water temperature, which might overshadow the effect of zooplankton, was overestimated. Thus, it seems safe to say that the dynamics of zooplankton has affected LNRPS/LNRPE.

The above discussion on how to interpret the negative correlation between LNRPS/LNRPE and temperature is based on the hypothesis that the optimal growth temperature is 16.2°C (Takasuka et al. 2007) while the temperature in this study ranged from 17.9 to 19.7°C (Fig. 11). However, a recent study suggested that the optimal growth temperature is higher than 16.2°C. Sakamoto et al. (2022) estimated that the metabolically optimal temperature of sardine larvae is 20.5°C by using a metabolic proxy which is the proportion of metabolically derived carbon in otolith carbonate and represents a proxy of the field metabolic rate. This result is consistent with a previous study that found high growth rates of larvae in waters around 20—21°C (Itoh et al. 2011). If the optimal growth temperature is around 20°C, then the negative correlation between LNRPS/LNRPE and temperature cannot be explained by a physiological effect on growth rate. At present, it is difficult to further statistically discuss the issue of whether food availability (bottom-up process) or water temperature (physiological process) drives zooplankton dynamics, but we look forward to advances in physiological research in the future.

The interannual variation in zooplankton density did not completely explain the interannual variation in recruitment. There are 4 possible reasons that why interannual variations in LNRPS and LNRPE do not perfectly match with the interannual variation in zooplankton density. The first reason is that the interannual variation in recruitment is not solely influenced by the feeding environment during the larval stage. As we have already mentioned, previous studies have suggested that temperature fluctuations impact the larval growth rate via metabolism (Takasuka et al. 2007, Sakamoto et al. 2022). A Granger causality test, using the water temperature model, did not deny the effect of interannual variation in water temperature. Additionally, there is a possibility that a density effect exists for Japanese sardine growth, as noted by Kamimura et al. (2022), who found that growth has declined with stock increases during the recent period of stock increase. The observation that an increase in sardine

abundance leads to a decrease in zooplankton has been documented in the Kuroshio—Oyashio transition region (Tadokoro et al. 2005, Kodama et al. 2022). Therefore, competition for food is expected to impact growth and survival. In this study, we focus solely on the passive transport stage. Therefore, we do not discuss the period after the juvenile stage when the fish start to migrate to the Kuroshio—Oyashio transition region. However, previous studies suggest the potential for strong density effects occurring after the juvenile stage. Apart from this, there is also a hypothesis that fluctuations in predator populations influence recruitment (Kawai & Isibasi 1979).

The second reason why interannual variations in LNRPS and LNRPE do not perfectly match with the interannual variation in zooplankton density is the variation in spawning grounds and season. We set the spawning grounds in 130—141° E and 29—36° N for the particle-tracking experiments. While this area almost covers the past spawning grounds, the actual spawning ground location varies drastically from year to year. For example, the gravity centers of the longitude and latitude of the spawning grounds were 132.0° E and 31° N in 1994, and 137.5° E and 34.5° N in 2010 (Nishikawa 2019), indicating that main larval feeding grounds might shift over 600 km from year to year. In addition, while we focused on the peak spawning season from January to April, spawning occurs in other seasons, and the egg number in other seasons have also varied year to year (Oozeki et al. 2007). Our ideal spawning grounds and season can reproduce the decadal-scale feeding grounds, but may miss the yearly variation. We used the ideal spawning grounds in this study for the purpose of reproducing the past feeding grounds including the period during which the spawning-ground survey had not been organized. It is necessary to reproduce more realistic feeding environments by using the detailed recent spawning-ground data for the next step. Furthermore, it has been pointed out that since 2004, the spawning grounds and spawning season have undergone significant changes, shifting from western to eastern Japan, and spawning is occurring earlier. As a result, it is believed that the probability of encountering predators has also changed compared to the past (Niino et al. 2021). Therefore, there is a possibility that explaining the variability in LNRPS solely based on the feeding environment fluctuations as before 2004 may no longer be feasible.

The third reason is the reliability of the LNRPS before 1975. From 1976, RPS is estimated using virtual population analysis based on age composition data from catch records. On the other hand, for the period

before 1975, since age composition data are unavailable, the estimates are derived from the egg number. There is no significant difference in the estimates between the overlapping periods of these 2 estimation methods (Fig. 3). However, the reliability of LNRPS before 1975 is not entirely guaranteed. For instance, notable peaks in LNRPS are observed in 1971 and 1973, but considering the occurrence of significant year classes in 1972 and 1974 (Hiramoto 1974, Kuroda 2007), it is possible that the LNRPS values for those years were higher. However, despite the possibility of year to year LNRPS estimates deviating from the true values, the analysis using the data set from Yatsu et al. (2005), which remains the only available data set for estimating LNRPS before 1975, holds significance. Previous studies have not denied the connection between early 1970s recruitment success and the subsequent increase in resource abundance in the late 1970s and beyond. Thus, the correlation between LNRPS fluctuations on a multi-year scale and zooplankton concentration variations is considered solid. In addition, we conducted Granger causality tests for both combined data from 1967 and new data from 1976. The zooplankton density showed Granger causality for both data sets.

The fourth reason is the reproducibility of the model itself. The output of this model is on a monthly basis, investigating the feeding environment using monthly flow fields. Cushing (1974, 1975, 1990) suggested that recruitment success depends on the match—mismatch between spawning time and phytoplankton bloom because the first-feeding planktonic larvae have not yet fully developed their foraging abilities and are most vulnerable to starvation. In the case of Japanese sardine, the spawning grounds are located in an area influenced by the Kuroshio Current, so it is believed that the eggs drift while hatching. Therefore, in this study, particle tracking was conducted, and the ambient zooplankton density during the tracking period was considered as the larval food availability. However, as mentioned in the previous section, this study conducted particle-tracking experiments by ideal spawning grounds and seasons and monthly flow field. Therefore, if the actual recruitment is determined by the impact of match—mismatch with food availability within 1 mo, we would be unable to reproduce or discuss such a short-term impact.

The results of this study do not dismiss other factors influencing stock fluctuation. However, the findings from the main transport routes of sardine larvae obtained in this study, which show higher (lower) zooplankton density during the period of increasing (decreasing) stock, suggest the possibility that the feeding environment around the Kuroshio axis during winter and spring may have influenced the recruitment success through the survival of larvae at least until 1996. While zooplankton density fluctuations do not explain the year to year variations of LNRPS/LNRPE, they might have acted as triggers for the resource increase at the end of the 1960s and the subsequent resource decrease at the end of the 1980s.

The increase in p-values of the Granger causality tests including the recent years (Table 1) implied that the effect of zooplankton on LNRPS has been weak (or absent) recently. There are 2 possible reasons for this. While the food environment is crucial, recent spawning grounds have shifted unusually eastward and spawning is occurring earlier, as reported by Niino et al. (2021). Therefore, there is a possibility that the zooplankton density, widely averaged from historically suggested spawning grounds and periods, is now substantially different from the current feeding environment. Regarding this possibility, detailed spawning ground data since 1979 and the availability of satellite chlorophyll data since 1997 may allow for a fairly accurate estimation of plankton density in the distribution area of larvae. This is an important issue for future consideration. However, a recent study reported that the relationship between growth rate and recruitment has disappeared since the late 1990s (Furuichi et al. 2020). The authors suggested that the disappearance of the relationship between growth rate and recruitment may be attributed to a decrease in predation pressure and/or the achievement of an optimal level of growth rate where the benefits of faster growth diminish. If there is no relationship between growth rate and recruitment, it is natural that the relationship between food availability and recruitment would also be absent.

4.3. Underlying mechanism of bottom-up control

Many studies have been conducted on the nutrient supply mechanisms of the Kuroshio main stream, which is the focus of this research. In the upstream Kuroshio region (around 131–138° E), where seafloor topography drastically changes, the island mass effect near Tokara strait (Hasegawa et al. 2021) and Izu ridge (Tanaka et al. 2019) supplies a huge amount of nutrients to the surface layer by vertical turbulent mixing and increases the primary production (Kobari et al. 2020). Turbulence is also caused by banded internal wave shear amplified between the Kuroshio and the continental slope and causes a large diapycnal diffusive nitrate flux to the surface layer (Nagai et

al. 2019). In the downstream Kuroshio region, the mesoscale subduction/obduction and near-inertial motions could catalyze double-diffusive favorable conditions and enhance the nutrient supply below 150 m near the front (Nagai et al. 2015). Additionally, a simulation study demonstrated that the interannual variation in winter MLD along the Kuroshio affects the zooplankton density through nutrient supply (Nishikawa et al. 2013b).

These studies mentioned above suggest the direct impact of the Kuroshio on the lower trophic level ecosystem. For example, in the Tokara Strait, it is known that the Kuroshio path varies with the Kuroshio transport (Nakamura et al. 2006), and the nutrient supply occurring during the encounter of the Kuroshio with rocky reefs should be influenced by such variations. The winter MLD interannual variation depends on the Kuroshio velocity (Nishikawa & Yasuda 2011). The interannual variation in Kuroshio transport and velocity is induced by the wind system change in the central Pacific (Nonaka et al. 2006). Although further research is necessary to elucidate the linkage among the Kuroshio, zooplankton density, and interannual variation in the Japanese sardine stock, it is possible that global-scale climate variations are influencing the fluctuations in sardine resources through bottom-up control as suggested by many previous studies (e.g. Kawasaki 1983).

LITERATURE CITED

Chavez FP, Messié M (2009) A comparison of Eastern Boundary Upwelling Ecosystems. Prog Oceanogr 83:80—96

Cushing DH (1974) The natural regulation of fish populations. In: Harden Jones FR (ed) Sea fisheries research. Elek Science, London, p 399—412

Cushing DH (1975) Marine ecology and fisheries. Cambridge University Press, New York, NY

Cushing DH (1990) Plankton production and year-class strength in fish populations: an update of the match/mismatch hypothesis. Adv Mar Biol 26:249—293

Furuichi S, Niino Y, Kamimura Y, Yukami R (2020) Time-varying relationships between early growth rate and recruitment in Japanese sardine. Fish Res 232:105723

Furuichi S, Yukami R, Kamimura Y, Nishijima S, Watanabe R (2022) Stock assessment and evaluation for Japanese sardine (fiscal year 2021). Marine fisheries stock assessment and evaluation for Japanese waters. FRA-SA2022-AC-01. Japan Fisheries Agency and Japan Fisheries Research and Education Agency, Tokyo. https://abchan.fra.go.jp/wpt/wp-content/uploads/2023/07/details_2022_01.pdf (in Japanese)

Granger CWJ (1969) Investigating causal relations by econometric models and cross-spectral methods. Econometrica 37:424—438

Hasegawa D, Matsuno T, Tsutsumi E, Senjyu T and others (2021) How a small reef in the Kuroshio cultivates the ocean. Geophys Res Lett 48:e2020GL092063

Hiramoto H (1974) The recent stock variations of Japanese sardine. Bull Jpn Soc Fish Oceanogr 25:151—156 (in Japanese)

Hurtt GC, Armstrong RA (1996) A pelagic ecosystem model calibrated with BATS data. Deep Sea Res II 43:653—683

Ichii T, Nishikawa H, Mahapatra K, Okamura H and others (2018) Oceanographic factors affecting interannual recruitment variability of Pacific saury (*Cololabis saira*) in the central and western North Pacific. Fish Oceanogr 27:445—457

Ito S (1961) Fisheries biology of the sardine, *Sardinops melanostictus* (T. & S.), in the waters around Japan. Bull Jpn Sea Reg Fish Natl Fish Res Lab 9:1—227 (in Japanese with English abstract)

Itoh S, Yasuda I, Nishikawa H, Sasaki H, Sasai Y (2009) Transport and environmental temperature variability of eggs and larvae of the Japanese anchovy (*Engraulis japonicus*) and Japanese sardine (*Sardinops melanostictus*) in the western North Pacific estimated via numerical particle-tracking experiments. Fish Oceanogr 18:118—133

Itoh S, Saruwatari T, Nishikawa H, Yasuda I and others (2011) Environmental variability and growth histories of larval Japanese sardine (*Sardinops melanostictus*) and Japanese anchovy (*Engraulis japonicus*) near the frontal area of the Kuroshio. Fish Oceanogr 20:114—124

Itoh S, Yasuda I, Saito H, Tsuda A, Komatsu K (2015) Mixed layer depth and chlorophyll *a*: profiling float observations in the Kuroshio—Oyashio Extension region. J Mar Syst 151:1—14

Ivanov AN (1992) Raspregelenie i Otzenka Chislennoisti Seboletkov Sarkinui v 1989g. Prog Rep 22nd Meet Jpn Russia Joint Res: Saury, Mackerel, Sardine, Squid and Pollock. Japan Fisheries Agency, Tokyo (in Russian with Japanese translation)

Kamimura Y, Tadokoro K, Furuichi S, Yukami R (2022) Stronger density-dependent growth of Japanese sardine with lower food availability: comparison of growth and zooplankton biomass between a historical and current stock-increase period in the western North Pacific. Fish Res 255:106461

Kasai A (1996) Transport and survival of Japanese sardine larvae (*Sardinops melanostictus*) in the Kuroshio—Oyashio region: a numerical approach. In: Wataname Y, Yamashita Y, Oozeki Y (eds) Survival strategies in early life stages of marine resources. A.A. Balkema, Rotterdam, p 219—226

Kawai H (1972) Hydrography of the Kuroshio Extension. In: Stommel H, Yoshida K (eds) Kuroshio, its physical aspects. University of Tokyo Press, Tokyo, p 235—352

Kawai T, Isibasi K (1979) A study of comparative biology of Japanese Pisces to population analysis. III. A quantitative analysis of early-stage mortality caused by cannibalism. Bull Tokai Reg Fish Res Lab 100:79—89

Kawasaki T (1983) Why do some pelagic fishes have wide fluctuations in their numbers? FAO Fish Rep 291:1065—1080

Kikuchi H, Konishi Y (1990) Monthly egg productions of the Japanese sardine, anchovy, and mackerels of the south-

ern coast of Japan by egg censuses: January 1987 through December 1988. Japan Fisheries Agency, Tokyo (in Japanese with English abstract)

Kinoshita T (1998) Northward migration of juveniles in the Kuroshio Extension. In: Watanabe Y, Wada T (eds) Stock fluctuations and ecological changes of the Japanese sardine. Koseisha-Koseikaku, Tokyo, p 84–92 (in Japanese)

Kobari T, Honma T, Hasegawa H, Yoshie N and others (2020) Phytoplankton growth and consumption by microzooplankton stimulated by turbulent nitrate flux suggest rapid trophic transfer in the oligotrophic Kuroshio. Biogeosciences 17:2441–2452

Kodama T, Igeta Y, Iguchi N (2022) Long-term variation in mesozooplankton biomass caused by top-down effects: a case study in the coastal Sea of Japan. Geophys Res Lett 49:e2022GL099037

Kuroda K (1991) Studies on the recruitment process focusing on the early life history of the Japanese sardine, *Sardinops melanostictus* (Schlegel). Bull Natl Res Inst Fish Sci 3:25–278

Kuroda K (2005) Foreboding increase of the Japanese sardine stock during the 1960s. Kuroshio no shigen kaiyō kenkyū (Fisheries biology and oceanography in the Kuroshio) 6:1–11 (in Japanese with English abstract)

Kuroda K (2007) Population increasing processes of Japanese sardine. Nippon Suisan Gakkaishi 73:750–753 (in Japanese)

Kuroda H, Saito T, Kage T, Takasuka A, Kamimura Y, Furuichi S, Nakanowatari T (2020) Unconventional sea surface temperature regime around Japan in the 2000s–2010s: potential influences on major fisheries resources. Front Mar Sci 7:574904

Liu S, Liu Y, Alabia ID, Tian Y and others (2020) Impact of climate change on wintering ground of Japanese anchovy (*Engraulis japonicus*) using marine geospatial statistics. Front Mar Sci 7:604

Lluch-Cota SE (2013) Modeling sardine and anchovy low-frequency variability. Proc Natl Acad Sci USA 110: 13240–13241

Ministry of Agriculture, Forestry and Fisheries Japan (2023) Statistics on marine fishery production. https://www.e-stat.go.jp/en/statistics/00500216 (accessed 29 January 2023)

Morimoto H, Kitajima S, Takahashi T, Goto T, Iguchi N (2023) Comparison of diets between larval Japanese sardine *Sardinops melanostictus* and Japanese anchovy *Engraulis japonicus* captured simultaneously around the Noto Peninsula, southern Japan Sea. Bull Jpn Soc Fish Oceanogr 87: 77–92

Nagai T, Inoue R, Tandon A, Yamazaki H (2015) Evidence of enhanced double-diffusive convection below the main stream of the Kuroshio Extension. J Geophys Res Oceans 120:8402–8421

Nagai T, Durán GS, Otero DA, Mori Y and others (2019) How the Kuroshio Current delivers nutrients to sunlit layers on the continental shelves with aid of near-inertial waves and turbulence. Geophys Res Lett 46:6726–6735

Nakamura H, Yamashiro T, Nishina A, Ichikawa H (2006) Time frequency variability of Kuroshio meanders in Tokara Strait. Geophys Res Lett 33:L21605

Nakano H, Tsujino H, Hirabara M, Yasuda T, Motoi T, Ishii M, Yamanaka G (2011) Uptake mechanism of anthropogenic CO_2 in the Kuroshio extension region in an ocean general circulation model. J Oceanogr 67:765–783

Nakano H, Ishii M, Rodgers KB, Tsujino H, Yamanaka G (2015) Anthropogenic CO_2 uptake, transport, storage, and dynamical controls in the ocean imposed by the meridional overturning circulation: a modeling study. Global Biogeochem Cycles 29:1706–1724

Nakata K, Hidaka K (2003) Decadal-scale variability in the Kuroshio marine ecosystem in winter. Fish Oceanogr 12: 234–244

Nakata K, Koyama S, Matsukawa Y (2001) Interannual variation in spring biomass and gut content composition of copepods in the Kuroshio current, 1971–89. Fish Oceanogr 10:329–341

Niino Y, Furuichi S, Kamimura Y, Yukami R (2021) Spatiotemporal spawning patterns and early growth of Japanese sardine in the western North Pacific during the recent stock increase. Fish Oceanogr 30:643–652

Nishikawa H (2019) Relationship between recruitment of Japanese sardine (*Sardinops melanostictus*) and environment of larval habitat in the low stock period (1995–2010). Fish Oceanogr 28:131–142

Nishikawa H, Yasuda I (2008) Japanese sardine (*Sardinops melanostictus*) mortality in relation to the winter mixed layer depth in the Kuroshio Extension region. Fish Oceanogr 17:411–420

Nishikawa H, Yasuda I (2011) Long-term variability of winter mixed layer depth and temperature along the Kuroshio jet in a high-resolution ocean general circulation model. J Oceanogr 67:503–518

Nishikawa H, Yasuda I, Itoh S (2011) Impact of winter-to-spring environmental variability along the Kuroshio jet on the recruitment of Japanese sardine (*Sardinops melanostictus*). Fish Oceanogr 20:570–582

Nishikawa H, Yasuda I, Itoh S, Komatsu K, Sasaki H, Sasai Y, Oozeki Y (2013a) Transport and survival of Japanese sardine (*Sardinops melanostictus*) eggs and larvae via particle tracking experiments. Fish Oceanogr 22:509–522

Nishikawa H, Yasuda I, Komatsu K, Sasaki H, Sasai Y, Setou T, Shimizu M (2013b) Winter mixed layer depth and spring bloom along the Kuroshio front: implications for the Japanese sardine stock. Mar Ecol Prog Ser 487:217–229

Nonaka M, Nakamura H, Tanimoto Y, Kagimoto T, Sasaki H (2006) Decadal variability in the Kuroshio–Oyashio Extension simulated in an eddy-resolving OGCM. J Clim 19:1970–1989

Noto M, Yasuda I (1999) Population decline of the Japanese sardine, *Sardinops melanostictus*, in relation to sea surface temperature in the Kuroshio Extension. Can J Fish Aquat Sci 56:973–983

Noto M, Yasuda I (2003) Empirical biomass model for the Japanese sardine, *Sardinops melanostictus*, with sea surface temperature in the Kuroshio Extension. Fish Oceanogr 12: 1–9

Odate K (1994) Zooplankton biomass and its long-term variation in the north Pacific Ocean, Tohoku sea area, Japan. Bull Tohoku Natl Fish Res Inst 56:115–173 (in Japanese with English Abstract)

Ohshimo S, Tanaka H, Hiyama Y (2009) Long-term assessment and growth changes of the Japanese sardine (*Sardinops melanostictus*) in the Sea of Japan and East China Sea from 1953 to 2006. Fish Oceanogr 18:346–358

Okazaki Y, Tadokoro K, Kubota H, Kamimura Y, Hidaka K (2019) Dietary overlap and optimal prey environments of larval and juvenile sardine and anchovy in the mixed water region of the western North Pacific. Mar Ecol Prog Ser 630:149–160

Okimoto T (2010) Econometric analysis of time-series with economic and financial data. Asakura Publishing, Tokyo (in Japanese)

Oozeki Y, Takasuka A, Kubota H, Barange M (2007) Characterizing spawning habitats of Japanese sardine (*Sardinops melanostictus*), Japanese anchovy (*Engraulis japonicus*), and Pacific round herring (*Etrumeus teres*) in the northwestern Pacific. CCOFI Rep 48:191−203

Orr JC, Najjar RG, Aumont O, Bopp L and others (2017) Biogeochemical protocols and diagnostics for the CMIP6 Ocean Model Intercomparison Project (OMIP). Geosci Model Dev 10:2169−2199

Polovina JJ, Mitchum GT, Evans GT (1995) Decadal and basin-scale variation in mixed layer depth and the impact on biological production in the Central and North Pacific, 1960−88. Deep Sea Res I 42:1701−1716

Rykaczewski RR, Checkley DM Jr (2008) Influence of ocean winds on the pelagic ecosystem in upwelling regions. Proc Natl Acad Sci USA 105:1965−1970

Sakamoto T, Takahashi M, Chung MT, Rykaczewski RR and others (2022) Contrasting life-history responses to climate variability in eastern and western North Pacific sardine populations. Nat Commun 13:5298

Sakuramoto K (2021) Reproductive success in fish stocks can be reproduced by environmental factors alone. Open Access Libr J 8:1−9

Shannon LJ, Field JG, Moloney CL (2004) Simulating anchovy−sardine regime shifts in the southern Benguela ecosystem. Ecol Modell 172:269−281

Sugisaki H (1996) Distribution of larval and juvenile Japanese sardine (*Sardinops melanostictus*) in the western North Pacific and its relevance to predation on these stages. In: Watanabe Y, Yamashita Y, Oozeki Y (eds) Survival strategies in early life stages of marine resources. A. A. Balkema, Rotterdam, p 261−270

Tadokoro K, Chiba S, Ono T, Midorikawa T, Saino T (2005) Interannual variation in *Neocalanus* biomass in the Oyashio waters of the western North Pacific. Fish Oceanogr 14:210−222

Takasuka A, Oozeki Y, Aoki I (2007) Optimal growth temperature hypothesis: Why do anchovy flourish and sardine collapse or vice versa under the same ocean regime? Can J Fish Aquat Sci 64:768−776

Takasuka A, Nishikawa H, Furuichi S, Yukami R (2021) Revisiting sardine recruitment hypotheses: egg-production-based survival index improves understanding of recruitment mechanisms of fish under climate variability. Fish Fish 22: 974−986

Tanaka T, Hasegawa D, Yasuda I, Tsuji H, Fujio S, Goto Y, Nishioka J (2019) Enhanced vertical turbulent nitrate flux in the Kuroshio across the Izu Ridge. J Oceanogr 75:195−203

Teske PR, Emami-Khoyi A, Golla TR, Sandoval-Castillo J and others (2021) The sardine run in southeastern Africa is a mass migration into an ecological trap. Sci Adv 7: eabf4514

Tsujino H, Nakano H, Sakamoto K, Urakawa S, Hirabara M, Ishizaki H, Yamanaka G (2017) Reference manual for the Meteorological Research Institute Community Ocean Model version 4 (MRI.COMv4). Tech Rep 80. Meteorological Research Institute, Tsukuba, doi:10.11483/mritechrepo.80

Tsujino H, Nakano H, Sakamoto K, Urakawa LS and others (2024) Impact of increased horizontal resolution of an ocean model on carbon circulation in the North Pacific Ocean. J Adv Model Earth Syst 16:e2023MS003720

Tsukamoto Y, Zenitani H, Kimura R, Watanabe Y, Oozeki Y (2001) Vertical distribution of fish larvae in the Kuroshio and Kuroshio−Oyashio transition region in early summer. Bull Natl Res Inst Fish Sci 16:39−56

Uotani I, Nakanishi A, Sakamoto H (1988) Feeding habit of Japanese sardine larvae. In: Kawaguchi K (ed) Exploitation of marine communities. Education Ministry, Tokyo, p 73−83 (in Japanese)

Urakawa LS, Tsujino H, Nakano H, Sakamoto K, Yamanaka G, Toyoda T (2020) The sensitivity of a depth-coordinate model to diapycnal mixing induced by practical implementations of the isopycnal tracer diffusion scheme. Ocean Modell 154:101693

Usui N, Wakamatsu T, Tanaka Y, Hirose N and others (2017) Four-dimensional variational ocean reanalysis: a 30-year high-resolution dataset in the western North Pacific (FORA-WNP30). J Oceanogr 73:205−233

Wada T, Jacobson LD (1998) Regimes and stock−recruitment relationships in Japanese sardine (*Sardinops melanostictus*), 1951−1995. Can J Fish Aquat Sci 55:2455−2463

Watanabe Y, Zenitani H, Kimura R (1995) Population decline of the Japanese sardine, *Sardinops melanostictus* owing to recruitment failures. Can J Fish Aquat Sci 52: 1609−1616

Yasuda I, Sugisaki H, Watanabe Y, Minobe SS, Oozeki Y (1999) Interdecadal variations in Japanese sardine and ocean/climate. Fish Oceanogr 8:18−24

Yatsu A, Watanabe T, Ishida M, Sugisaki H, Jacobson LD (2005) Environmental effects on recruitment and productivity of Japanese sardine *Sardinops melanostictus* and chub mackerel *Scomber japonicus* with recommendations for management. Fish Oceanogr 14:263−278

Yukimoto S, Kawai H, Koshiro T, Oshima N and others (2019) The Meteorological Research Institute Earth System Model Version 2.0, MRI-ESM2.0: description and basic evaluation of the physical component. J Meteor Soc Jpn 97:931−965